Inorg. Chem. **2003**, *42*, 5085–5096

An ^{17}O NMR and Quantum Chemical Study of Monoclinic and Orthorhombic Polymorphs of Triphenylphosphine Oxide

David L. Bryce,[†] Klaus Eichele,[‡] and Roderick E. Wasylishen*[,†]

Department of Chemistry, University of Alberta, Edmonton, Alberta, Canada T6G 2G2, and Institut für Anorganische Chemie, Universität Tübingen, Auf der Morgenstelle 18, 72076 Tübingen, Germany

Received December 6, 2002

Solid-state ^{17}O NMR spectroscopy is employed to characterize powdered samples of known monoclinic and orthorhombic modifications of ^{17}O-enriched triphenylphosphine oxide, Ph_3PO. Precise data on the orientation-dependent ^{17}O electric field gradient (EFG) and chemical shift (CS) tensors are obtained for both polymorphs. While the ^{17}O nuclear quadrupolar coupling constants (C_Q) are essentially identical for the two polymorphs ($C_Q = -4.59 \pm 0.01$ MHz (orthorhombic); $C_Q = -4.57 \pm 0.01$ MHz (monoclinic)), the spans (Ω) of the CS tensors are distinctly different ($\Omega = 135 \pm 3$ ppm (orthorhombic); $\Omega = 155 \pm 5$ ppm (monoclinic)). The oxygen CS tensor is discussed in terms of Ramsey's theory and the electronic structure of the phosphorus–oxygen bond. The NMR results favor the hemipolar σ-bonded $R_3P^+–O^-$ end of the resonance structure continuum over the multiple bond representation. Indirect nuclear spin–spin (**J**) coupling between ^{31}P and ^{17}O is observed directly in ^{17}O magic-angle-spinning (MAS) NMR spectra as well as in ^{31}P MAS NMR spectra. Ab initio and density-functional theory calculations of the ^{17}O EFG, CS, and $^1J(^{31}P,^{17}O)$ tensors have been performed with a variety of basis sets to complement the experimental data. This work describes an interesting spin system for which the CS, quadrupolar, **J**, and direct dipolar interactions all contribute significantly to the observed ^{17}O NMR spectra and demonstrates the wealth of information which is available from NMR studies of solid materials.

Introduction

The information available from previous NMR studies on phosphine oxides, their complexes, and their derivatives has generally been restricted to the determination of isotropic ^{31}P and ^{17}O chemical shifts (CS), δ_{iso}, and isotropic J coupling constants from solution NMR spectroscopy,[1−11] as well as $\delta_{iso}(^{31}P)$ from ^{31}P magic-angle spinning (MAS) NMR spectroscopy in the solid state.[12−15] Some information on the ^{31}P ($I = 1/2$) CS tensor is also available.[16−25] In contrast, results from ^{17}O ($I = 5/2$) NMR spectroscopy of phosphine oxides in the solid state are lacking. The range of oxygen isotropic

* To whom correspondence should be addressed. E-mail: Roderick.Wasylishen@UAlberta.ca. Phone: 780-492-4336. Fax: 780-492-8231.

† University of Alberta.

‡ Universität Tübingen.

(1) Pomerantz, M.; Terrazas, M. S.; Cheng, Y.; Gu, X. *Phosphorus, Sulfur Silicon* **1996**, *109−110*, 505−508.
(2) Grossmann, G.; Gruner, M.; Seifert, G. *Z. Chem.* **1976**, *16*, 362−363.
(3) Gray, G. A.; Albright, T. A. *J. Am. Chem. Soc.* **1977**, *99*, 3243−3250.
(4) Dahn, H.; Toan, V. V.; Ung-Truong, M.-N. *Magn. Reson. Chem.* **1992**, *30*, 1089−1096.
(5) Christ, H. A.; Diehl, P. *Helv. Phys. Acta* **1963**, *36*, 170−182.
(6) Christ, H. A.; Diehl, P.; Schneider, HR.; Dahn, H. *Helv. Chim. Acta* **1961**, *44*, 865−880.
(7) Quin, L. D.; Szewczyk, J.; Linehan, K.; Harris, D. L. *Magn. Reson. Chem.* **1987**, *25*, 271−273.
(8) Szewczyk, J.; Linehan, K.; Quin, L. D. *Phosphorus Sulfur* **1988**, *37*, 35−40.
(9) McFarlane, H. C. E.; McFarlane, W. *J. Chem. Soc., Chem. Commun.* **1978**, 531−532.
(10) Hibbert, R. C.; Logan, N. *J. Chem. Soc., Dalton Trans.* **1985**, 865−866.
(11) Evans, S. A., Jr. In *^{17}O NMR Spectroscopy in Organic Chemistry*; Boykin, D. W., Ed.; CRC Press: Boca Raton, FL, 1991; Chapter 10.
(12) Davies, J. A.; Dutremez, S.; Pinkerton, A. A. *Inorg. Chem.* **1991**, *30*, 2380−2387.
(13) Calcagno, P.; Kariuki, B. M.; Kitchin, S. J.; Robinson, J. M. A.; Philp, D.; Harris, K. D. M. *Chem. Eur. J.* **2000**, *6*, 2338−2349.
(14) Arumugam, S.; Glidewell, C.; Harris, K. D. M. *J. Chem. Soc., Chem. Commun.* **1992**, 724−726.
(15) Lynch, D. E.; Smith, G.; Byriel, K. A.; Kennard, C. H. L.; Kwiatkowski, J.; Whittaker, A. K. *Aust. J. Chem.* **1997**, *50*, 1191−1194.
(16) Lagier, C. M.; Scheler, U.; McGeorge, G.; Sierra, M. G.; Olivieri, A. C.; Harris, R. K. *J. Chem. Soc., Perkin Trans 2* **1996**, 1325−1329.
(17) Apperley, D. C.; Chaloner, P. A.; Crowe, L. A.; Harris, R. K.; Harrison, R. M.; Hitchcock, P. B.; Lagier, C. M. *Phys. Chem. Chem. Phys.* **2000**, *2*, 3511−3518.
(18) Hargé, J.-C.; El Abdallaoui, H. E. A.; Rubini, P. *Magn. Reson. Chem.* **1993**, *31*, 752−757.

10.1021/ic020706p CCC: $25.00
Published on Web 07/26/2003

chemical shifts in solution is on the order of 2500 ppm with phosphine oxides generally falling in the range of 20−100 ppm.[26−28] Overviews of ^{17}O nuclear quadrupolar coupling constants (C_Q), which are very sensitive to the electric field gradient (EFG) about the ^{17}O nucleus, are available.[29−31] Values of $C_Q(^{17}O)$ range from less than 1.0 MHz (e.g., MoO_4^{2-}) to greater than 15 MHz (e.g., H_2O_2).

The focus of this work is to characterize the anisotropic oxygen NMR interaction tensors for the prototypal terminal oxygen in the PO bonding environment in the solid state. The ^{17}O NMR spectra of the $^{31}P-^{17}O$ spin pair in solid triphenylphosphine oxide, Ph_3PO, should in principle provide a rare opportunity where one must consider all four fundamental NMR interactions simultaneously when carrying out spectral simulations. For the $^{31}P-^{17}O$ spin pair, these interactions are the following: (i) the ^{17}O quadrupolar interaction; (ii) the ^{17}O chemical shift interaction; (iii) the direct dipolar coupling interaction between ^{17}O and ^{31}P; (iv) the indirect nuclear spin−spin (**J**) coupling interaction between ^{17}O and ^{31}P. Given the number of parameters which will be indicative of the bonding environment at oxygen, ^{17}O solid-state NMR spectroscopy should provide an important perspective on the nature of the phosphorus−oxygen bond, a topic of ongoing debate.[32−41] While solid-state ^{31}P NMR studies have been employed extensively to characterize the PO bond of phosphine oxides, equivalent investigations on the terminal partner are lacking. In principle, oxygen should be better suited to investigate the nature of the PO bond because, to a first approximation, its NMR properties will be affected less by the substituents at phosphorus. In practice, the experimental difficulties of ^{17}O solid-state NMR as compared to ^{31}P may have prevented such studies hitherto.

Ph_3PO is known to exist as several different polymorphs and pseudopolymorphs[42−48] and is also useful as a crystallization aid for many organic compounds.[49] Polymorphism refers to the ability of a compound to crystallize in more than one distinct crystal structure, and pseudopolymorphism refers to compounds which may crystallize with a water molecule or other solvate incorporated into the crystal structure.[50] The problem of crystal structure prediction (CSP) from a molecular formula is rendered much more difficult as a result of the possibility of polymorphism.[51,52] Solid-state NMR spectroscopy is an important tool for studying polymorphs.[53−60] This study aims to determine the sensitivity of the EFG, CS, and **J** tensors of a quadrupolar nucleus, ^{17}O, to polymorphism, namely in the orthorhombic and monoclinic polymorphs of Ph_3PO. Furthermore, a qualitative interpretation of the resulting NMR parameters will be provided.

To supplement the experimental data, restricted Hartree−Fock (RHF), hybrid B3LYP density functional theory (DFT), multiconfigurational self-consistent field (MCSCF), and zeroth-order regular approximation (ZORA) DFT calculations of the oxygen nuclear magnetic shielding tensor, EFG

(19) Rubini, P.; El Alaoui El Abdallaoui, H. *Phosphorus, Sulfur Silicon* **1994**, *97*, 57−61.
(20) Lagier, C. M.; Olivieri, A. C.; Harris, R. K. *J. Chem. Soc., Perkin Trans. 2* **1998**, 1791−1796.
(21) Dutasta, J. P.; Robert, J. B.; Wiesenfeld, L. In *Phosphorus Chemistry: Proceedings of the 1981 International Conference*; Quin, L. D., Verkade, J. G., Eds.; ACS Symposium Series 171; American Chemical Society: Washington, DC, 1981; pp 581−584.
(22) Bemi, L.; Clark, H. C.; Davies, J. A.; Fyfe, C. A.; Wasylishen, R. E. *J. Am. Chem. Soc.* **1982**, *104*, 438−445.
(23) El Alaoui El Abdallaoui, H.; Rubini, P. *Spectrochim. Acta A* **1993**, *49*, 329−338.
(24) Montana, A. J.; Zumbulyadis, N.; Dailey, B. P. *J. Am. Chem. Soc.* **1977**, *99*, 4290−4293.
(25) Robert, J. B.; Wiesenfeld, L. *Mol. Phys.* **1981**, *44*, 319−327.
(26) Berger, S.; Braun, S.; Kalinowski, H.-O. *NMR Spectroscopy of the Non-Metallic Elements*; Becconsall, J., English language translation; John Wiley & Sons: Chichester, U.K., 1997; Chapter 5.
(27) (a) Gerothanassis, I. P.; Momenteau, M. *J. Am. Chem. Soc.* **1987**, *109*, 6944−6947. (b) Gerothanassis, I. P.; Momenteau, M.; Loock, B. *J. Am. Chem. Soc.* **1989**, *111*, 7006−7012.
(28) McFarlane, W.; McFarlane, H. C. E. In *Multinuclear NMR*; Mason, J., Ed.; Plenum: New York, 1987; Chapter 14.
(29) Gerothanassis, I. P. In *Encyclopedia of Nuclear Magnetic Resonance*; Grant, D. M., Harris, R. K., Eds.; Wiley Inc.: Chichester, U.K., 1996; pp 3430−3440.
(30) Kintzinger, J. P. In *NMR of Newly Accessible Nuclei*; Laszlo, P., Ed.; Academic Press: New York, 1983; Chapter 4.
(31) Butler, L. G. In *^{17}O NMR Spectroscopy in Organic Chemistry*; Boykin, D. W., Ed.; CRC Press: Boca Raton, FL, 1991; Chapter 1.
(32) Gilheany, D. G. In *The Chemistry of Organophosphorus Compounds, Volume 2: Phosphine Oxides, Sulphides, Selenides and Tellurides*; Hartley, F. R., Ed.; John Wiley and Sons: Chichester, U.K., 1992; Chapter 1.
(33) Burford, N. *Coord. Chem. Rev.* **1992**, *112*, 1−18.
(34) Schmidt, M. W.; Gordon, M. S. *J. Am. Chem. Soc.* **1985**, *107*, 1922−1930.
(35) Rai, U. S.; Symons, M. C. R. *J. Chem. Soc., Faraday Trans.* **1994**, *90*, 2649−2652.
(36) Chesnut, D. B. *J. Am. Chem. Soc.* **1998**, *120*, 10504−10510.
(37) Gilheany, D. G. *Chem. Rev.* **1994**, *94*, 1339−1374.
(38) See, R. F.; Dutoi, A. D.; Fettinger, J. C.; Nicastro, P. J.; Ziller, J. W. *J. Chem. Crystallogr.* **1998**, *28*, 893−898.
(39) Sandblom, N.; Ziegler, T.; Chivers, T. *Can. J. Chem.* **1996**, *74*, 2363−2371.
(40) Cooper, D. L.; Cunningham, T. P.; Gerratt, J.; Karadakov, P. B.; Raimondi, M. *J. Am. Chem. Soc.* **1994**, *116*, 4414−4426.
(41) Dobado, J. A.; Martínez-García, H.; Molina, J. M.; Sundberg, M. R. *J. Am. Chem. Soc.* **1998**, *120*, 8461−8471.
(42) Brock, C. P.; Schweizer, W. B.; Dunitz, J. D. *J. Am. Chem. Soc.* **1985**, *107*, 6964−6970.
(43) Thomas, J. A.; Hamor, T. A. *Acta Crystallogr.* **1993**, *C49*, 355−357.
(44) Spek, A. L. *Acta Crystallogr.* **1987**, *C43*, 1233−1235.
(45) Baures, P. W.; Silverton, J. V. *Acta Crystallogr.* **1990**, *C46*, 715−717.
(46) Ruban, G.; Zabel, V. *Cryst. Struct. Commun.* **1976**, *5*, 671−677.
(47) Gusev, A. I.; Bokii, N. G.; Afonina, N. N.; Timofeeva, T. V.; Kalinin, A. E.; Struchkov, Yu. T. *J. Struct. Chem. (Engl.Transl.)* **1973**, *14*, 101−108; *Zh. Strukt. Khim.* **1973**, *14*, 115−125.
(48) Bandoli, G.; Bortolozzo, G.; Clemente, D. A.; Croatto, U.; Panattoni, C. *J. Chem. Soc. A* **1970**, 2778−2780.
(49) Etter, M. C.; Baures, P. W. *J. Am. Chem. Soc.* **1988**, *110*, 639−640.
(50) (a) Bernstein, J.; Davey, R. J.; Henck, J.-O. *Angew. Chem., Int. Ed.* **1999**, *38*, 3440−3461. (b) Dunitz, J. D.; Bernstein, J. *Acc. Chem. Res.* **1995**, *28*, 193−200.
(51) Desiraju, G. R. *Nat. Mater.* **2002**, *1*, 77−79.
(52) Desiraju, G. R. *Science* **1997**, *278*, 404−405.
(53) Harris, R. K. In *Encyclopedia of Nuclear Magnetic Resonance*; Grant, D. M., Harris, R. K., Eds.; Wiley Inc.: Chichester, U.K., 1996; pp 3734−3740.
(54) Padden, B. E.; Zell, M. T.; Dong, Z.; Schroeder, S. A.; Grant, D. J. W.; Munson, E. J. *Anal. Chem.* **1999**, *71*, 3325−3331.
(55) Liang, J.; Ma, Y.; Chen, B.; Munson, E. J.; Davis, H. T.; Binder, D.; Chang, H.-T.; Abbas, S.; Hsu, F.-L. *J. Phys. Chem. B* **2001**, *105*, 9653−9662.
(56) Sidhu, P. S.; Enright, G. D.; Ripmeester, J. A.; Penner, G. H. *J. Phys. Chem. B* **2002**, *106*, 8569−8581.
(57) Harper, J. K.; Facelli, J. C.; Barich, D. H.; McGeorge, G.; Mulgrew, A. E.; Grant, D. M. *J. Am. Chem. Soc.* **2002**, *124*, 10589−10595.
(58) Medek, A.; Frydman, L. *J. Am. Chem. Soc.* **2000**, *122*, 684−691.
(59) Middleton, D. A.; Le Duff, C. S.; Peng, X.; Reid, D. G.; Saunders, D. *J. Am. Chem. Soc.* **2000**, *122*, 1161−1170.
(60) Apperley, D. C.; Fletton, R. A.; Harris, R. K.; Lancaster, R. W.; Tavener, S.; Threlfall, T. L. *J. Pharm. Sci.* **1999**, *88*, 1275−1280.

tensor, and the oxygen−phosphorus **J** coupling tensor have been carried out.

Theory and Experimental Strategy

Under conditions of high-power ^{1}H decoupling, the ^{31}P−^{17}O spin pair of Ph_3PO may be considered as "isolated". Four NMR interaction tensors influence the ^{17}O NMR line shape: the chemical shift tensor, $\boldsymbol{\delta}$, the indirect nuclear spin−spin coupling tensor, **J**, the electric field gradient (EFG) tensor, **V**, and the direct dipolar coupling tensor, **D**. The **D** and **J** tensors also explicitly involve the spin-coupled ^{31}P nucleus. If only the symmetric parts of $\boldsymbol{\delta}$ and **J** are considered, then each of these tensors may possess up to three unique principal components: δ_{11}, δ_{22}, δ_{33}; J_{11}, J_{22}, J_{33}. The span of the chemical shift tensor is defined as[61]

$$\Omega = \delta_{11} - \delta_{33} \tag{1}$$

and the skew is defined as

$$\kappa = \frac{3(\delta_{22} - \delta_{iso})}{\Omega} \tag{2}$$

The isotropic values, δ_{iso} and J_{iso}, are simply the averages of the principal components. Since the **V** tensor has zero trace, its magnitude is described by two parameters, the nuclear quadrupolar coupling constant, $C_Q = eV_{ZZ}Q/h$, and the quadrupolar asymmetry parameter, $\eta = (V_{XX} - V_{YY})/V_{ZZ}$, where V_{ZZ} is the largest component of the EFG tensor. The **D** tensor also has zero trace and is axially symmetric in the absence of motion and thus has a magnitude which may be denoted by the direct dipolar coupling constant, R_{DD}:

$$R_{DD} = \frac{\mu_0}{4\pi}\frac{\hbar}{2\pi}\gamma_P\gamma_O\langle r_{PO}^{-3}\rangle \tag{3}$$

Here γ_P and γ_O are the magnetogyric ratios for ^{31}P and ^{17}O, 10.8394×10^7 and -3.62808×10^7 rad s^{-1} T^{-1}, respectively.[62] The motionally averaged inverse cube of the phosphorus−oxygen internuclear distance is given by $\langle r_{PO}^{-3}\rangle$.

The definition of the orientation of each of the four interaction tensors in the molecular framework requires additional parameters. To define as completely as possible the magnitude and orientation of the oxygen NMR interaction tensors ($\boldsymbol{\delta}$, **V**, **D**, and **J**), four methods are combined.

(i) First, ^{17}O NMR spectra of MAS samples yield δ_{iso}, C_Q, η, and J_{iso} via analysis of the second-order quadrupolar line shape of the ^{17}O central transition.[63] No orientation information is gained.

(ii) Second, ^{31}P NMR spectra of MAS samples provide the magnitude and absolute sign of $C_Q(^{17}O)$ through measurement of the residual dipolar coupling, d:[97]

$$d = -\frac{3C_Q|R_{eff}|}{20|\nu_S|}(3\cos^2\beta^D - 1 + \eta\sin^2\beta^D\cos 2\alpha^D) \tag{4}$$

Here, ν_S is the Larmor frequency of ^{17}O, R_{eff} is the effective dipolar coupling constant (eq 5, vide infra), and α^D and β^D are polar angles which define the orientation of the dipolar coupling tensor in the principal axis system (PAS) of the EFG tensor for ^{17}O. The **D** and **J** tensors are assumed to share the same PAS in eq 4. In this study, this is a valid assumption (vide infra). Slow-spinning ^{31}P MAS NMR spectra also allow for the establishment of the relative signs of R_{eff} and J_{iso} by analyzing the six subspectra resulting from the interplay of ^{31}P CS anisotropy and ^{31}P,^{17}O dipolar and indirect couplings.[64]

(iii) With the knowledge of the parameters listed in parts i and ii, simulation of ^{17}O NMR spectra of stationary samples provides the three principal components of the oxygen chemical shift tensor as well as the orientation of this tensor with respect to the ^{17}O EFG tensor. The Euler angles α, β, and γ are used to define the counterclockwise (mathematically positive) rotations required to bring the PAS of the EFG tensor into coincidence with the PAS of the CS tensor. The angle β is the simplest to visualize and simply represents the angle between the z-axes of the two coordinate systems.

(iv) Ab initio calculations of the $\boldsymbol{\delta}$, **V**, and **J** tensors, in conjunction with the orientation information gained from the stationary samples, allow for the proposal of absolute orientations of all of the tensors in the molecular framework. Information on the principal components of **J** is also gained. Knowledge of the principal components of **J** is important due to the relationship between R_{DD}, the anisotropy in **J** ($\Delta J = J_{33} - (J_{11} + J_{22})/2$), and the effective dipolar coupling constant observed in an NMR experiment, R_{eff}:[65]

$$R_{eff} = R_{DD} - \Delta J/3 \tag{5}$$

Experimental and Computational Procedures

(i) Sample Preparation. The preparation of phosphine oxides from the corresponding phosphines is generally straightforward; however, if ^{17}O enrichment is required, it may be necessary to modify existing procedures depending on the source(s) of ^{17}O available.[29] In the present case, H_2O (37.5% ^{17}O, Isotec) was used to introduce the label via hydrolysis of dibromotriphenylphosphorane, formed during the direct bromination of triphenylphosphine.[66] In a typical reaction, 1.5 g of triphenylphosphine was dissolved in 20 mL of dichloromethane, and the solution was cooled by stirring in an ice bath. The stoichiometric amount of bromine, 0.91 g, was dissolved in 20 mL of dichloromethane, and the solution was added dropwise under continued cooling. Then, the solution was allowed to warm to room temperature and the labeled water was added directly and stirred for 30 min. Initially, the water formed a separate phase but disappeared quickly to give a clear solution. The dichloromethane solution was then washed twice with a solution of Na_2CO_3 in regular water and, after separation of the layers, dried

(61) Mason, J. *Solid State Nucl. Magn. Reson.* **1993**, *2*, 285−288.
(62) Mills, I.; Cvitaš, T.; Homann, K.; Kallay, N.; Kuchitsu, K. *Quantities, Units and Symbols in Physical Chemistry*, 2nd ed.; Blackwell Science: Oxford, U.K., 1993.
(63) Eichele, K.; Wasylishen, R. E.; Nelson, J. H. *J. Phys. Chem. A* **1997**, *101*, 5463−5468.
(64) (a) VanderHart, D. L.; Gutowsky, H. S.; Farrar, T. C. *J. Chem. Phys.* **1969**, *50*, 1058−1065. (b) Harris, R. K.; Packer, K. J.; Thayer, A. M. *J. Magn. Reson.* **1985**, *62*, 284−297. (c) Grimmer, A.-R.; Neels, J. *Z. Anorg. Allg. Chem.* **1989**, *576*, 117−130.
(65) Wasylishen, R. E. In *Encyclopedia of Nuclear Magnetic Resonance*; Grant, D. M., Harris, R. K., Eds.; Wiley Inc.: Chichester, U.K., 1996; pp 1685−1695.
(66) Hays, H. R.; Peterson, D. J. In *Organic Phosphorus Compounds*; Kosolapoff, G. M., Maier, L., Eds.; Wiley-Interscience: New York, 1972; Vol. 3, Chapter 6.

over $MgSO_4$. The product was then crystallized from the dichloromethane solution or, after removal of the solvent, from acetone.

Samples were recrystallized from acetone to provide the monoclinic polymorph and from dichloromethane to provide the orthorhombic polymorph. In addition to redetermining the structures of monoclinic and orthorhombic polymorphs by single-crystal X-ray diffraction, unit cell parameters were also routinely checked by single-crystal X-ray diffraction on selected crystals after recrystallization to confirm the identity of the particular polymorphs being investigated by solid-state NMR spectroscopy.

(ii) X-ray Crystallography. Triphenylphosphine oxide was recrystallized from dichloromethane to yield a colorless needle−plate crystal having approximate dimensions of $0.10 \times 0.17 \times 0.27$ mm. This sample, polymorph A, was found to crystallize in a primitive orthorhombic cell, space group *Pbca*. Lattice parameters obtained, $a = 11.273(6)$ Å, $b = 29.115(3)$ Å, and $c = 9.154(4)$ Å, are in good agreement with those reported previously.[42,43,48]

Triphenylphosphine oxide was recrystallized from acetone to yield a colorless needle crystal having approximate dimensions of $0.12 \times 0.17 \times 0.50$ mm. This sample, polymorph B, was found to crystallize in a primitive monoclinic cell, space group $P2_1/c$. Lattice parameters obtained, $a = 11.068(1)$ Å, $b = 8.731(2)$ Å, $c = 16.274(1)$ Å, and $\beta = 107.919(6)°$, are in good agreement with those reported previously.[42]

The X-ray crystal structures for both polymorphs indicate a single unique molecule in the asymmetric unit. Furthermore, crystal symmetry does not place any restrictions on the orientations or asymmetries of the NMR interaction tensors. All NMR spectra were interpreted with this knowledge in mind.

(iii) Solid-State NMR Spectroscopy. All solid-state NMR spectra were obtained at ambient temperature. All ^{17}O solid-state NMR spectra for polymorphs A and B were recorded using a one-pulse sequence with high-power proton decoupling on a Bruker AMX 400 spectrometer, $B_0 = 9.4$ T, operating at a frequency of 54.243 MHz. Spectra were referenced to the ^{17}O liquid water (natural abundance) signal at 0.00 ppm. Relaxation delays of a few seconds were employed. An MAS rate of 5.2 kHz was used to acquire 3000−4000 scans for both polymorphs of Ph_3PO packed into 7 mm o.d. zirconia rotors. For ^{17}O NMR spectra of stationary samples, 4000−8000 scans were acquired.

Phosphorus-31 MAS NMR spectra of polymorphs A and B were recorded using a 4 mm double-resonance MAS probe on a Chemagnetics CMX Infinity 200 spectrometer operating at a frequency of 81.02 MHz. A standard cross-polarization pulse sequence with two-pulse phase modulated (TPPM)[67] proton decoupling during acquisition was employed. A proton $\pi/2$ pulse of 2.40 μs, contact time of 3.7 ms, TPPM pulse length of 6.5 μs, acquisition time of 102.4 ms, and pulse delay of 120 s were used to acquire typically 500−1000 scans at MAS rates of 9−11 kHz.

All spectra were simulated using WSOLIDS,[68] an NMR simulation package developed in our laboratory which incorporates the POWDER algorithm of Alderman et al.[69]

(iv) Ab Initio Calculations. Calculations of EFG and nuclear magnetic shielding tensors were carried out using Gaussian 98 and Gaussian 98W[70] running on a 43P model 260 IBM RS 6000 workstation or a Dell Dimension personal computer (Pentium III, 550 MHz, 512 Mb RAM). Coordinates of P, O, and C atoms from single-crystal X-ray diffraction studies were employed in the calculations. Carbon−hydrogen bond lengths were set to 1.08 Å. Restricted Hartree−Fock (RHF) theory and density functional theory (DFT) with the B3LYP functional[71] were used in the calculations. Calculations of nuclear magnetic shielding tensors were performed using the GIAO (gauge-independent atomic orbitals) method.[72] Locally dense basis sets[73] were used in some cases. All basis sets (3-21G, 6-311G, 6-311+G*, 6-311++G**) were available within the Gaussian package. Calculated oxygen nuclear magnetic shielding tensors were converted to chemical shift tensors using our revised absolute shielding scale for oxygen,[74] whereby the following relationship is employed, with all quantities in ppm:

$$\delta = 287.5 - \sigma \qquad (6)$$

The nuclear quadrupolar coupling constants, C_Q, were determined from the calculated largest EFG component, V_{ZZ}, by means of the equation $C_Q = eV_{ZZ}Q/h$. Conversion of V_{ZZ} from atomic units to V m^{-2} was carried out by using the factor 9.7177×10^{21} V m^{-2} per au. The recommended value of the quadrupole moment, Q, for oxygen-17 is −25.58 mb;[75,76] this value has been used in this work.

MCSCF calculations of indirect nuclear spin−spin coupling tensors were carried out using the Dalton Quantum Chemistry Program[77] running on a 43P model 260 IBM RS 6000 workstation. The correlation-consistent basis sets of Dunning[78] available within the Dalton program were employed. Because ab initio calculations of **J** tensors require major computational resources, phosphine oxide (H_3PO), was used as a model system in many cases. The geometry of phosphine oxide was optimized at the MP2/6-311+G* level using Gaussian 98. The optimized structure has C_{3v} symmetry, a phosphorus−oxygen bond length of 1.4918 Å, a phosphorus−hydrogen bond length of 1.41 Å, and a H−P−O bond angle of 117.0°. This structure is in good agreement with the RHF/6-31G** and MP2/6-31G** optimized structures reported by Stewart and co-workers.[79] The geometry of trimethylphosphine oxide was also

(67) Bennett, A. E.; Rienstra, C. M.; Auger, M.; Lakshmi, K. V.; Griffin, R. G. *J. Chem. Phys.* **1995**, *103*, 6951−6958.

(68) Eichele, K.; Wasylishen, R. E. *WSOLIDS NMR Simulation Package*, version 1.17.26; 2000.

(69) Alderman, D. W.; Solum, M. S.; Grant, D. M. *J. Chem. Phys.* **1986**, *84*, 3717−3725.

(70) Frisch, M. J.; Trucks, G. W.; Schlegel, H. B.; Scuseria, G. E.; Robb, M. A.; Cheeseman, J. R.; Zakrzewski, V. G.; Montgomery, J. A.; Stratmann, R. E.; Burant, J. C.; Dapprich, S.; Millam, J. M.; Daniels, A. D.; Kudin, K. N.; Strain, M. C.; Farkas, O.; Tomasi, J.; Barone, V.; Cossi, M.; Cammi, R.; Mennucci, B.; Pomelli, C.; Adamo, C.; Clifford, S.; Ochterski, J.; Petersson, G. A.; Ayala, P. Y.; Cui, Q.; Morokuma, K.; Malick, D. K.; Rabuck, A. D.; Raghavachari, K.; Foresman, J. B.; Cioslowski, J.; Ortiz, J. V.; Stefanov, B. B.; Liu, G.; Liashenko, A.; Piskorz, P.; Komaromi, I.; Gomperts, R.; Martin, R. L.; Fox, D. J.; Keith, T.; Al-Laham, M. A.; Peng, C. Y.; Nanayakkara, A.; Gonzalez C.; Challacombe, M.; Gill, P. M. W.; Johnson, B. G.; Chen, W.; Wong, M. W.; Andres, J. L.; Head-Gordon, M.; Replogle, E. S.; Pople, J. A. *Gaussian 98*, revision A.7; Gaussian, Inc.: Pittsburgh, PA, 1998.

(71) Becke, A. D. *J. Chem. Phys.* **1993**, *98*, 5648−5652.

(72) (a) Ditchfield, R. *Mol. Phys.* **1974**, *27*, 789−807. (b) Wolinski, K.; Hinton, J. F.; Pulay, P. *J. Am. Chem. Soc.* **1990**, *112*, 8251−8260.

(73) (a) Chesnut, D. B.; Moore, K. D. *J. Comput. Chem.* **1989**, *10*, 648−659. (b) Chesnut, D. B.; Rusiloski, B. E.; Moore, K. D.; Egolf, D. A. *J. Comput. Chem.* **1993**, *14*, 1364−1375.

(74) Wasylishen, R. E.; Bryce, D. L. *J. Chem. Phys.* **2002**, *117*, 10061−10066.

(75) Sundholm, D.; Olsen, J. *J. Phys. Chem.* **1992**, *96*, 627−630.

(76) (a) Pyykkö, P. *Mol. Phys.* **2001**, *19*, 1617−1629. (b) Pyykkö, P. *Z. Naturforsch.* **1992**, *47a*, 189−196.

(77) Helgaker, T.; Jensen, H. J. Aa.; Jørgensen, P.; Olsen, P. J.; Ruud, K.; Ågren, H.; Andersen, H. T.; Bak, K. L.; Bakken, V.; Christiansen, O.; Dahle, P.; Dalskov, E. K.; Enevoldsen, T.; Fernandez, B.; Heiberg, H.; Hettema, H.; Jonsson, D.; Kirpekar, S.; Kobayashi, R.; Koch, H.; Mikkelsen, K. V.; Norman, P.; Packer, M. J.; Saue, T.; Taylor, P. R.; Vahtras, O. *Dalton: An electronic structure program*, release 1.0; 1997.

(78) (a) Dunning, T. H., Jr. *J. Chem. Phys.* **1989**, *90*, 1007−1023. (b) Woon, D. E.; Dunning, T. H., Jr. *J. Chem. Phys.* **1995**, *103*, 4572−4585. (c) Woon, D. E.; Dunning, T. H., Jr. *J. Chem. Phys.* **1993**, *98*, 1358−1371.

optimized at the MP2/6-311+G* level using Gaussian 98. Two different active spaces were used for the MCSCF wave functions. Both calculations employ C_s symmetry. The first is based on a complete active space (CAS) denoted 52/51, where the first two numbers denote active orbitals of a′ and a″ symmetry and the latter two numbers denote the inactive orbitals of a′ and a″ symmetry. This CAS wave function is essentially analogous to a Hartree−Fock wave function. A larger restricted active space (RAS) wave function denoted 52/52/00/51 was also used, where the four sets of numbers denote RAS1, RAS2, RAS3, and inactive orbitals of a′ and a″ symmetry. All coupling mechanisms (Fermi-contact (FC), spin-dipolar (SD), diamagnetic spin−orbital (DSO), and paramagnetic spin−orbital (PSO)) were included in the calculations.

Relativistic DFT calculations of $\mathbf{J}(^{31}\mathrm{P},^{17}\mathrm{O})$ were carried out using the ZORA approach of Autschbach and Ziegler,[80] implemented in the NMR spin−spin coupling module[81] of the Amsterdam Density Functional (ADF) package.[82] These calculations were also carried out on the IBM workstation, with basis sets which are available within the ADF package. The VWN[83] + Becke88[84] and Perdew86[85] generalized gradient approximations (GGA) were used to determine the unperturbed molecular orbitals, as described in reference 80. Both ZORA scalar and spin−orbit calculations were carried out. All calculations included the relativistic analogues of the FC, SD, DSO, and PSO coupling mechanisms.

Results and Discussion

(i) Solid-State NMR Spectroscopy. *(a) Magic-Angle Spinning NMR.* Shown in Figures 1 and 2 are the experimental ^{17}O NMR spectra of MAS samples of the two polymorphs of ^{17}O-enriched Ph_3PO obtained at 9.4 T, along with simulated spectra which employ the parameters given in Table 1. These spectra provide δ_{iso}, the magnitude of C_Q, η, and the magnitude of $^1J_{iso}(^{31}\mathrm{P}, ^{17}\mathrm{O})$. The second-order quadrupolar interaction dominates the observed central 1/2 ↔ −1/2 transition line shapes; however, indirect spin−spin coupling between oxygen and phosphorus is also clearly evident in both of these spectra. This coupling manifests itself as a sharp splitting equal to J_{iso}, about 150 Hz at the discontinuities in the spectra. Discrepancies in the relative intensities of the two main discontinuities of the powder patterns are attributed to the moderate MAS rate employed, 5.2 kHz.

The information obtained concerning the oxygen EFG tensor, $|C_Q| = 4.59$ MHz for the orthorhombic form and 4.57 MHz for the monoclinic form, may be compared to nuclear quadrupole resonance (NQR) data reported by Brown and Cheng at 77 K, $|C_Q| = 4.683(2)$ MHz.[86,87] Certainly vibrational or librational effects on the EFG tensor as a result of the reduced temperature used in these studies could be partly responsible for the discrepancy of ∼2%.[42,88,89] Which polymorph of Ph_3PO that was studied via NQR is not indicated; however, the reported nonzero asymmetry parameter (0.085(15)) suggests that it is not the orthorhombic form. Our ambient-temperature NMR studies have provided values of <0.01 and 0.030 ± 0.002 for the ^{17}O quadrupolar asymmetry parameters of the orthorhombic and monoclinic forms, respectively. To our knowledge, the largest experi-

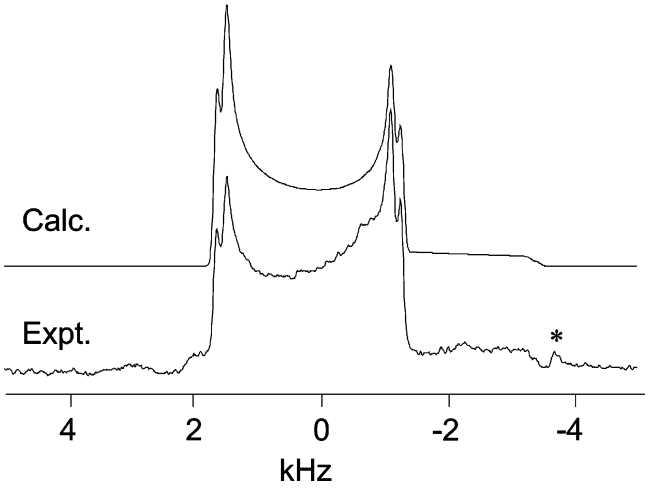

Figure 1. Experimental and simulated ^{17}O MAS NMR spectra of triphenylphosphine oxide-*^{17}O* (37.5%) recrystallized from dichloromethane (orthorhombic, polymorph A) acquired at $B_0 = 9.4$ T and $\nu_{rot} = 5.2$ kHz. A spinning sideband is indicated by the asterisk.

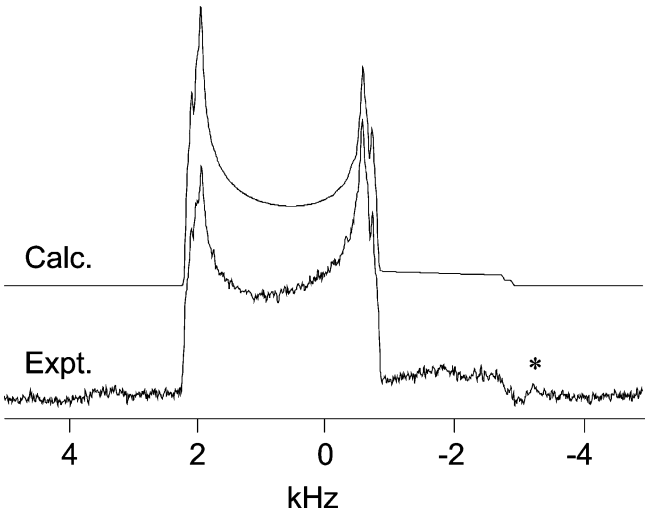

Figure 2. Experimental and simulated ^{17}O MAS NMR spectra of triphenylphosphine oxide-*^{17}O* (37.5%) recrystallized from acetone (monoclinic, polymorph B) acquired at $B_0 = 9.4$ T and $\nu_{rot} = 5.2$ kHz. A spinning sideband is indicated by the asterisk.

(79) Stewart, E. L.; Nevins, N.; Allinger, N. L.; Bowen, J. P. *J. Org. Chem.* **1997**, *62*, 5198−5207.
(80) (a) Autschbach, J.; Ziegler, T. *J. Chem. Phys.* **2000**, *113*, 936−947. (b) Autschbach, J.; Ziegler, T. *J. Chem. Phys.* **2000**, *113*, 9410−9418.
(81) (a) Dickson, R. M.; Ziegler, T. *J. Phys. Chem.* **1996**, *100*, 5286−5290. (b) Khandogin, J.; Ziegler, T. *Spectrochim. Acta, Part A* **1999**, *55*, 607−624.
(82) (a) *ADF*, version 2000.01; Theoretical Chemistry, Vrije Universiteit: Amsterdam; http://www.scm.com. (b) Baerends, E. J.; Ellis, D. E.; Ros, P. *Chem. Phys.* **1973**, *2*, 41−51. (c) Versluis, L.; Ziegler, T. *J. Chem. Phys.* **1988**, *88*, 322−328. (d) te Velde, G.; Baerends, E. J. *J. Comput. Phys.* **1992**, *99*, 84−98. (e) Fonseca Guerra, C.; Snijders, J. G.; te Velde, G.; Baerends, E. J. *Theor. Chem. Acc.* **1998**, *99*, 391−403.
(83) Vosko, S. H.; Wilk, L.; Nusair, M. *Can. J. Phys.* **1980**, *58*, 1200−1211.
(84) Becke, A. D. *Phys. Rev. A* **1988**, *38*, 3098−3100.
(85) Perdew, J. P. *Phys. Rev. B* **1986**, *33*, 8822−8824; **1986**, *34*, 7406.
(86) Brown, T. L.; Cheng, C. P. *Faraday Symp. Chem. Soc.* **1978**, *13*, 75−82.
(87) Cheng, C. P.; Brown, T. L. *J. Am. Chem. Soc.* **1980**, *102*, 6418−6421.
(88) Lucken, E. A. C. In *Advances in Nuclear Quadrupole Resonance*; Smith, J. A. S., Ed.; John Wiley & Sons: Chichester, U.K., 1983; Vol. 5, Chapter 3.
(89) Dunitz, J. D.; Maverick, E. F.; Trueblood, K. N. *Angew. Chem., Int. Ed.* **1988**, *27*, 880−895.

Table 1. Oxygen-17 NMR Parameters for Solid Triphenylphosphine Oxide

	polymorph A, orthorhombic (recryst from dichloromethane)	polymorph B, monoclinic (recryst from acetone)
δ_{iso}/ppm	45.1 ± 0.2	53.0 ± 0.2
Ω/ppm	135 ± 3	155 ± 5
κ	−0.76 ± 0.03	−0.75 ± 0.02
δ_{11}/ppm	130	150
δ_{22}/ppm	11	14
δ_{33}/ppm	−5	−5
C_Q/MHz	−4.59 ± 0.01	−4.57 ± 0.01
η	<0.01	0.030 ± 0.002
α^a	*b*	66.5 ± 3.5
β	86.5 ± 0.5	86.3 ± 0.5
γ	6.5 ± 0.5	8.1 ± 0.5
R_{eff}/Hz	−1800 ± 100	−1800 ± 50
J_{iso}/Hz	150 ± 20	150 ± 20

[a] The Euler angles α, β, and γ define the counterclockwise rotations required to bring the PAS of the EFG tensor into coincidence with the PAS of the CS tensor. [b] The angle α is undefined for an axially symmetric EFG tensor.

mental ^{17}O quadrupolar coupling constant is that for the terminal oxygen nucleus in ozone (+19.96 MHz);[90] DFT calculations by Kaupp et al. predict similarly large values for dioxygen ligands bound to iron porphyrin model complexes.[91] Values for carbonyl oxygen nuclei, which are σ- and π-bonded to carbon, range from approximately 6.65 MHz in thymine[92] to 10.808 MHz in benzophenone.[93] The smaller values of $C_Q(^{17}O)$ in Ph_3PO are indicative of an oxygen environment which tends toward an isolated closed-shell oxygen atom, and therefore favors the $R_3P^+-O^-$ resonance contributor.

On the basis of a comparison of the NMR parameters available from the ^{17}O MAS spectra, it is apparent that the parameters δ_{iso} and η are the most sensitive to differences in the two polymorphs. The chemical shifts, 45.1 ± 0.2 ppm for the orthorhombic form and 53.0 ± 0.2 ppm for the monoclinic form, are significantly different. The oxygen chemical shift range for phosphine oxides, R_3PO, is about 20−100 ppm;[26] thus, the difference for the two polymorphs examined here is nearly 10% of the known range. With respect to the total known chemical shift range for oxygen, about 2500 ppm,[26,27] the variation seen here is very small. The quadrupolar asymmetry parameters for the two forms, 0.000 and 0.030, are significantly different. The nonzero asymmetry of the oxygen EFG tensor in the monoclinic form may be readily detected by visual inspection of the ^{17}O MAS NMR spectrum (Figure 2). Conversely, C_Q and J_{iso} are essentially identical for the monoclinic and orthorhombic forms. Thus, the latter parameters do not appear to be useful for distinguishing between polymorphs in this case.

Shown in Figure 3 are the experimental and simulated ^{31}P spectra of a MAS sample of Ph_3PO-*^{17}O* (30%) (orthorhombic form; monoclinic form not shown). The theory and experimental examples pertaining to the MAS spectra of a spin-

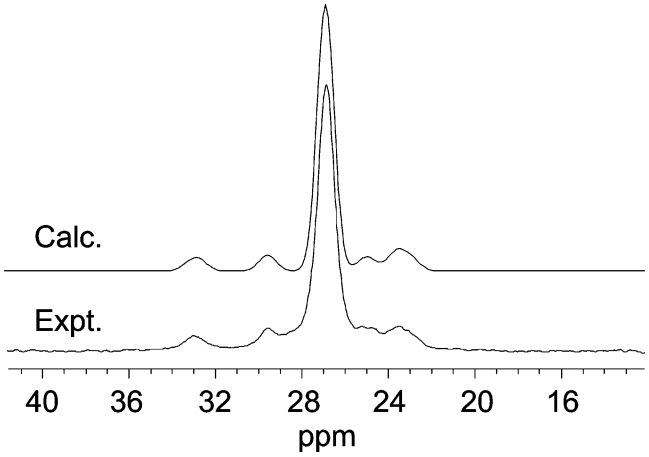

Figure 3. Experimental and simulated ^{31}P CPMAS NMR spectra of triphenylphosphine oxide-*^{17}O* (30%) recrystallized from dichloromethane (orthorhombic, polymorph A) acquired at B_0 = 4.7 T and ν_{rot} = 11.0 kHz.

$^1/_2$ nucleus spin−spin coupled to a quadrupolar nucleus with a nonzero EFG tensor have been discussed.[94−100] The intense peak in Figure 3 represents those ^{31}P nuclei which are adjacent to zero-spin oxygen isotopes. Simulation of the distortion of the multiplet in the ^{31}P MAS NMR spectrum provides the residual dipolar coupling constant, *d* (see eq 4), which indicates that $C_Q(^{17}O)$ is negative, and confirms the magnitude of $J_{iso}(^{31}P,^{17}O)$. The ^{31}P MAS NMR spectrum of a powder sample spinning sufficiently slowly, such that several spinning sidebands of significant intensity are observed, can yield information on the relative signs of R_{eff} and J_{iso}, in the present case even without a detailed analysis. While the ^{31}P CS tensor can be determined separately from the peaks of phosphorus coupled to NMR passive oxygen, the subspectra resulting from coupling to ^{17}O depend on the interplay of CS anisotropy with dipolar and indirect coupling, resulting in subspectra that are squeezed or expanded relative to the uncoupled phosphorus.[64] In the case of Ph_3PO, the high-frequency subspectra are squeezed, indicating that R_{eff} and J_{iso} have opposite signs. Under the assumption that $R_{eff} \approx R_{DD}$, and hence is negative, the absolute sign of J_{iso} is positive.

Reports on indirect nuclear spin−spin coupling (or "scalar" coupling) to the ^{17}O nucleus have been discussed and summarized.[26,28] The observation of *J* coupling to oxygen-17 is still considered somewhat rare due to rapid quadrupolar relaxation (self-decoupling) of the ^{17}O nucleus in solution[11,28] and broad lines dominated by the quadrupolar interaction in the solid state. Nevertheless, phosphine oxides and related

(90) Cohen, E. A.; Pickett, H. M. *J. Mol. Struct.* **1983**, *97*, 97−100.
(91) Kaupp, M.; Rovira, C.; Parrinello, M. *J. Phys. Chem. B* **2000**, *104*, 5200−5208.
(92) Wu, G.; Dong, S.; Ida, R. *Chem. Commun.* **2001**, 891−892.
(93) Scheubel, W.; Zimmerman, H.; Haeberlen, U. *J. Magn. Reson.* **1985**, *63*, 544−555.
(94) Hexem, J. G.; Frey, M. H.; Opella, S. J. *J. Chem. Phys.* **1982**, *77*, 3847−3856.
(95) Olivieri, A. C.; Frydman, L.; Diaz, L. E. *J. Magn. Reson.* **1987**, *75*, 50−62.
(96) Olivieri, A.; Frydman, L.; Grasselli, M.; Diaz, L. *Magn. Reson. Chem.* **1988**, *26*, 615−618.
(97) Olivieri, A. C. *J. Magn. Reson.* **1989**, *81*, 201−205.
(98) (a) Grasselli, M.; Diaz, L. E.; Olivieri, A. C. *Spectrosc. Lett.* **1991**, *24*, 895−907. (b) Eichele, K.; Wasylishen, R. E. *Solid State Nucl. Magn. Reson.* **1992**, *1*, 159−163. (c) Gan, Z.; Grant, D. M. *J. Magn. Reson.* **1990**, *90*, 522−534.
(99) Harris, R. K.; Olivieri, A. C. *Prog. NMR Spectrosc.* **1992**, *24*, 435−456.
(100) Eichele, K.; Wasylishen, R. E. *Inorg. Chem.* **1994**, *33*, 2766−2773.

compounds tend to give narrow enough lines in many cases in solution for $^1J_{iso}(^{31}P, ^{17}O)$ to be observed.[1,3,5,101,102] The result obtained here, 150 ± 20 Hz, is typical of known solution $^1J_{iso}(^{31}P, ^{17}O)$ values, which range from 81 Hz in PhHP(O)OH[4] to 220 Hz for the terminal oxygen atom in $(H_3CO)_2P(O)H$.[9] Solution NMR spectroscopy of Ph_3PO dissolved in chloroform-d_1 gives a value of 160 ± 2.4 Hz for $^1J(^{31}P, ^{17}O)_{iso}$.[103] Direct interpretation of the *J* coupling to give definitive information about the nature of the bonding between oxygen and phosphorus in phosphine oxides is difficult due to the complicated formulations of the Hamiltonians representing the various mechanisms contributing to the total **J** tensor. For example, there is no direct relationship between the magnitude of the coupling and bond length/strength; this is especially evident for couplings involving phosphorus.[104−106] Nevertheless, a comparison of the reduced isotropic coupling constants, K ($=4\pi^2 J/h\gamma_a\gamma_b$), for directly bonded $^{13}C-^1H$ (3.3×10^{20} N A^{-2} m^{-3} in alkanes), $^{31}P-^1H$ (3.9×10^{20} N A^{-2} m^{-3} in phosphane), $^{13}C-^{17}O$ (-5.4×10^{20} N A^{-2} m^{-3} in acetone), and $^{31}P-^{17}O$ (-22.7×10^{20} N A^{-2} m^{-3} in Ph_3PO) spin pairs demonstrates the disproportionately large reduced coupling for phosphorus and oxygen. However, the reduced isotropic chlorine−oxygen coupling constant in the perchlorate anion is even larger,[107] -53.5×10^{20} N A^{-2} m^{-3}. A further discussion of the nature of the phosphorus−oxygen coupling tensor is presented in the context of theoretical calculations (vide infra).

(b) NMR Spectroscopy of Stationary Powder Samples. The ^{17}O NMR spectra of stationary powdered samples of orthorhombic and monoclinic Ph_3PO (37.5% ^{17}O) are shown in Figures 4 and 5, respectively. Some loss of intensity due to nonuniform spectral excitation, especially for the monoclinic form (Figure 5), is evident near the high-frequency discontinuities. Nevertheless, accurate extraction of the NMR parameters is ensured by simulation of the positions of the spectral features along the frequency axis. In fact, the simulations of these spectra proved to be extremely sensitive to the relative orientations of the CS and EFG tensors; this is exemplified by the small errors in the Euler angles reported in Table 1. The angle α is undefined for an axially symmetric EFG tensor, as is the case for the orthorhombic polymorph.

The pronounced sensitivity of the simulated ^{17}O NMR spectra of stationary powdered samples to the relative orientations of the oxygen CS and EFG tensors is demonstrated with selected examples in Figure 6. Shown in Figure 6a is an expanded region of simulated spectra for the orthorhombic polymorph with all parameters as given in Table 1, except for the angle γ which is varied in small steps. Similarly in Figure 6b, the effect of varying the angle β upon simulated spectra of the monoclinic polymorph is shown. This series of simulated spectra is provided as additional evidence for the high precision to which the ^{17}O NMR interaction tensors have been determined for both polymorphs (Table 1).

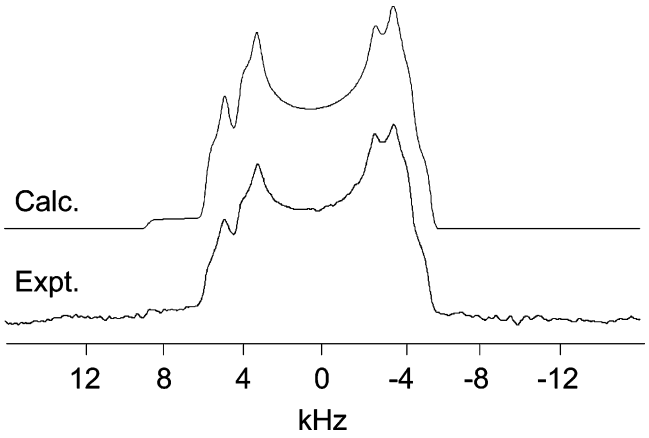

Figure 4. Experimental and simulated ^{17}O NMR spectra of a stationary sample of triphenylphosphine oxide-*^{17}O* (37.5%) recrystallized from dichloromethane (orthorhombic, polymorph A) acquired at $B_0 = 9.4$ T.

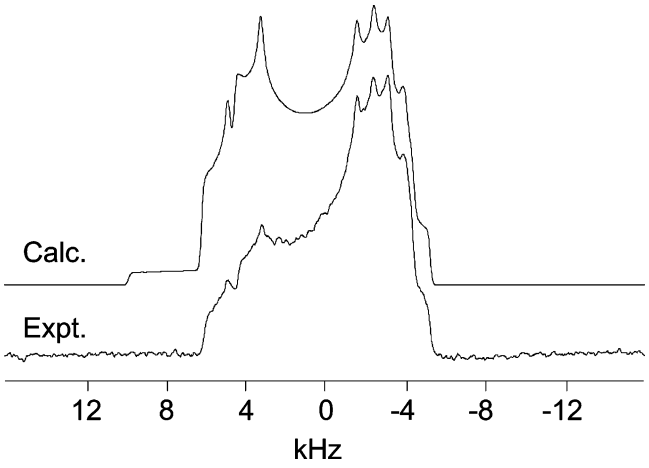

Figure 5. Experimental and simulated ^{17}O NMR spectra of a stationary sample of triphenylphosphine oxide-*^{17}O* (37.5%) recrystallized from acetone (monoclinic, polymorph B) acquired at $B_0 = 9.4$ T.

While the skews of the CS tensors are identical for the two polymorphs (−0.76), and clearly not axially symmetric in contrast to the EFG tensors, the spans are significantly different. The oxygen CS tensor spans, 135 and 155 ppm, are much smaller than those for carbonyl oxygen nuclei in organic compounds. For example, the span of the oxygen CS tensor in benzophenone-*^{17}O*, as determined by single-crystal NMR, is 1062 ppm.[93] Recent studies by Wu and coworkers on powdered samples have shown that the span of the oxygen CS tensor in amides generally ranges from 500 to 630 ppm,[108,109] although intermolecular hydrogen bonding

(101) Harris, R. K. *Nuclear Magnetic Resonance Spectroscopy: A Physicochemical View*; Longman: Malaysia, 1986; Section 5-12.
(102) Gerlt, J. A.; Demou, P. C.; Mehdi, S. *J. Am. Chem. Soc.* **1982**, *104*, 2848−2856.
(103) Sammons, R. D.; Frey, P. A.; Bruzik, K.; Tsai, M.-D. *J. Am. Chem. Soc.* **1983**, *105*, 5455−5461.
(104) Eichele, K.; Wasylishen, R. E.; Schurko, R. W.; Burford, N.; Whitla, W. A. *Can. J. Chem.* **1996**, *74*, 2372−2377.
(105) Karaghiosoff, K. In *Multiple Bonds and Low Coordination in Phosphorus Chemistry*; Regitz, M., Scherer, O. J., Eds.; G. Thieme Verlag: Stuttgart, Germany, 1990; pp 463−471.
(106) Gorenstein, D. G. In *Phosphorus-31 NMR: Principles and Applications*; Gorenstein, D. G., Ed.; Academic Press: New York, 1984; Chapter 2.
(107) Alei, M., Jr. *J. Chem. Phys.* **1965**, *43*, 2904−2906.
(108) Wu, G.; Yamada, K.; Dong, S.; Grondey, H. *J. Am. Chem. Soc.* **2000**, *122*, 4215−4216.
(109) Yamada, K.; Dong, S.; Wu, G. *J. Am. Chem. Soc.* **2000**, *122*, 11602−11609.

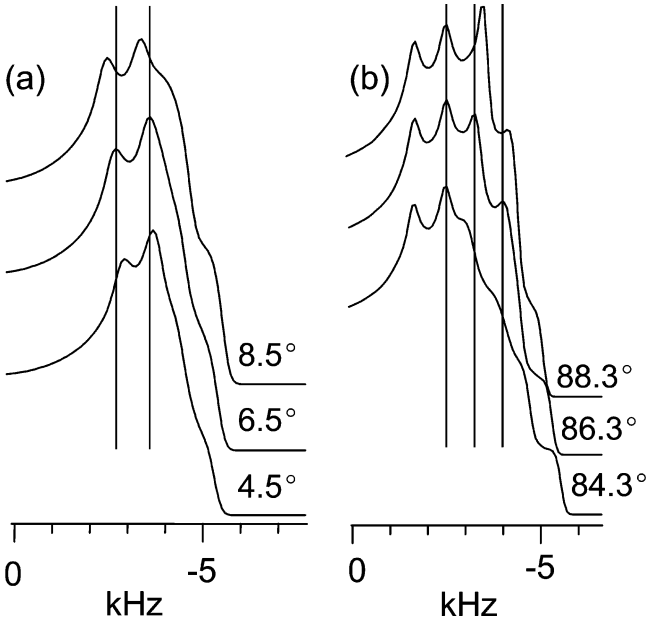

Figure 6. Examples of the pronounced dependence of the simulated ^{17}O line shape on the relative orientations of the CS and EFG tensors. (a) Selected region of simulated ^{17}O NMR spectra of the orthorhombic polymorph of Ph_3PO (see Figure 4) based on the parameters given in Table 1, with the Euler angle γ varied from 4.5 to 8.5°, is shown. The middle spectrum, $\gamma = 6.5°$, gives the best fit to the experimental spectrum. (b) Selected region of simulated ^{17}O NMR spectra of the monoclinic polymorph of Ph_3PO (see Figure 5) based on the parameters given Table 1, with the Euler angle β varied from 84.3 to 88.3°, is shown. The middle spectrum, $\beta = 86.3°$, gives the best fit to the experimental spectrum. A similar sensitivity is also seen corresponding to the angle β for the orthorhombic form and corresponding to the angle γ for the monoclinic form (Table 1). Vertical lines which pass through the discontinuities corresponding to the experimental spectra serve to emphasize the sensitivity of the simulated spectra to the angle variation.

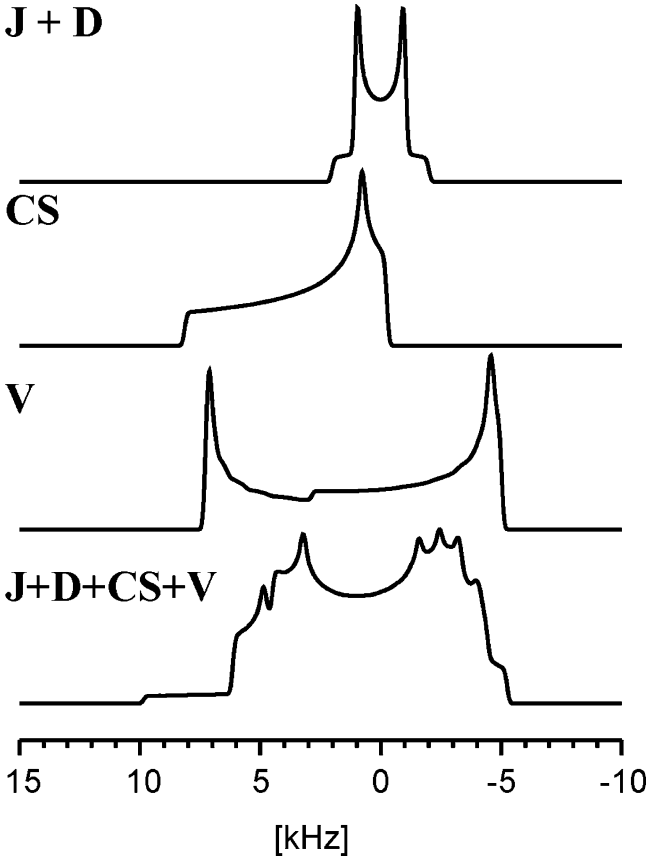

Figure 7. Simulated ^{17}O NMR spectra of the monoclinic polymorph of Ph_3PO showing the individual contributions of indirect and dipolar coupling (**J** + **D**), chemical shift anisotropy (CS), and quadrupolar coupling (**V**) to the static NMR line shape (bottom trace).

has been shown to lower this to 270 ppm in thymine.[92] Given the lack of such hydrogen bonding to oxygen in Ph_3PO, it seems that the values of Ω for terminal PO oxygen nuclei are intrinsically lower than those for terminal C=O oxygen nuclei. Ab initio calculations carried out by Power suggest this conclusion as well; the small span for the phosphine oxides was taken as an indication of a lack of multiple bonding character for the phosphorus and oxygen atoms.[110] The isotropic oxygen chemical shifts of the two polymorphs, 45.1 ppm (orthorhombic) and 53.0 ppm (monoclinic), may also be contrasted with those of carbonyl compounds, which range from ~350 to 600 ppm.[30]

To demonstrate how the individual NMR interactions contribute to the observed static ^{17}O NMR spectrum, we show in Figure 7 the spectra that would arise for indirect and dipolar coupling, CS, or quadrupolar interaction alone, as well as the sum of all contributions, using in each case the parameters for the monoclinic polymorph quoted in Table 1. Note that the total line shape has no resemblance to any of the individual contributions; i.e., the spectrum is not dominated by any single interaction. Accurate and precise determinations of the contributions due to each of the individual interactions is made possible through the systematic experimental strategy outlined above.

The differences between the terminal oxygen CS tensors for carbonyl groups and phosphine oxides may be understood in the context of Ramsey's theory of nuclear magnetic shielding,[111,112] which decomposes the total shielding tensor into diamagnetic (σ^d) and paramagnetic (σ^p) parts. The paramagnetic contribution, usually negative, is typically responsible for observed changes in chemical shifts for a given nucleus. The magnitude of σ^p depends on magnetic dipole-allowed mixing between the highest occupied molecular orbitals (MO) and low-lying virtual MOs with large contributions from the atomic orbitals of the atom of interest. Furthermore, the magnitude of σ^p is inversely related to the energy gap between the relevant occupied and virtual orbitals, with a smaller energy gap leading to larger paramagnetic deshielding. The required mixing may be visualized as rotations of an occupied orbital about one of the three Cartesian axes to produce constructive overlap with an appropriate virtual MO.

The oxygen chemical shift tensor in carbonyl compounds is dominated by a significant paramagnetic contribution which is usually attributed to magnetic-dipole-allowed

(110) Power, W. P. *J. Am. Chem. Soc.* **1995**, *117*, 1800−1806.

(111) Ramsey, N. F. *Molecular Beams*; Oxford University Press: London, 1956; pp 162−166, 208−213.

(112) (a) Ramsey, N. F. *Phys. Rev.* **1950**, *77*, 567. (b) Ramsey, N. F. *Phys. Rev.* **1950**, *78*, 699−703. (c) Ramsey, N. F. *Phys. Rev.* **1951**, *83*, 540−541. (d) Ramsey, N. F. *Phys. Rev.* **1952**, *86*, 243−246.

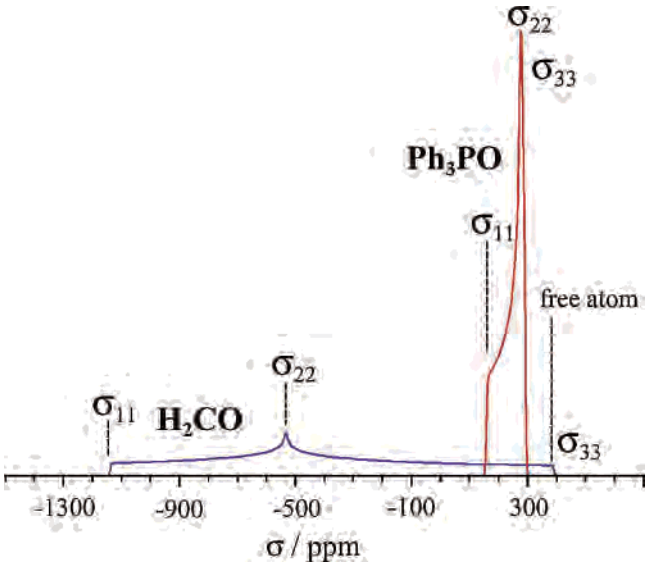

Figure 8. Comparison of the terminal oxygen magnetic shielding tensors in formaldehyde, H_2CO, and triphenylphosphine oxide, Ph_3PO. The oxygen shielding tensor in H_2CO is known to be strongly influenced by magnetic dipole allowed n → π^* mixing, which results in the strong paramagnetic deshielding particularly of σ_{11} as shown here. In contrast, all three components of the oxygen shielding tensor in Ph_3PO lack a significant paramagnetic contribution due to the lack of low-lying virtual orbitals of appropriate symmetry. See text for further discussion.

n → π^* mixing.[113] This mixing results in a particularly large deshielding along the C−O bond axis. Experimental data for the oxygen shielding tensor of formaldehyde, available from spin-rotation tensor measurements,[114,115] are presented in Figure 8. The span of the oxygen shielding tensor in formaldehyde is 1530 ppm. In contrast, all three experimental principal components of the oxygen shielding tensor for Ph_3PO are very close to the free atom value for oxygen, 395.1 ppm.[116] Comparison of the most deshielded components of the oxygen shielding tensors, as well as their overall spans, in formaldehyde and Ph_3PO, indicates immediately a distinct lack of significant paramagnetic contributions to the shielding tensor in the case of Ph_3PO. This may be attributed to a lack of availability of low-lying virtual orbitals of appropriate symmetry (e.g., π^* orbitals) with significant AO contributions from oxygen. This in turn provides some insight into the electronic structure of the PO bond and in particular lends support to the polarized singly σ-bonded $R_3P^+-O^-$ end of the resonance continuum. This is in agreement with the conclusions of Rai and Symons,[35] Dobado et al.,[41] and Chesnut,[36] who propose that a single polarized σ-bond, $R_3P^+-O^-$, is the most appropriate representation. Nevertheless, the present results do not conclusively rule out a small degree of π bonding as is advocated by e.g., Sandblom et al.[39] and See et al.[38]

A comparison of the observed effective dipolar coupling constant, $R_{eff} = -1800$ Hz, with the direct dipolar coupling constant, R_{DD}, determined from the X-ray bond length provides some insight into the magnitude and sign of the anisotropic portion of the indirect nuclear spin−spin coupling tensor, ΔJ. For the monoclinic form, the phosphorus−oxygen bond length of 1.485(2) Å[117] results in R_{DD} equal to -2016 ± 9 Hz. Motional averaging of about 11% would be required to fully account for the reduction of R_{DD} to −1800 Hz. Averaging of R_{DD} due to vibrational and librational motion in organic solids is known to be generally 1−4%[118−121] at 20 °C. On the basis of eq 5 and motional averaging on this order of magnitude, ΔJ is estimated to be −588 to −406 Hz. These values are in good agreement with ab initio calculations presented in the following section (vide infra). A greater degree of motional averaging would reduce the apparent magnitude of ΔJ. Regardless of the exact amount of vibrational averaging, the reduction in R_{DD} (rather than increase) indicates a negative value for ΔJ and suggests an upper limit on the order of −600 Hz.

(ii) Ab Initio and DFT Calculations: Comparison of Theory and Experiment. *(a) Oxygen-17 EFG and CS Tensors*. The results of restricted Hartree−Fock (RHF) and nonrelativistic DFT/B3LYP calculations of the ^{17}O CS and EFG tensors are summarized in Tables 2 and 3 for the orthorhombic and monoclinic forms of Ph_3PO, respectively. Also shown for comparison are the experimentally measured parameters determined in the present solid-state study. One striking aspect of the calculations is the lack of quantitative agreement between the experimental and theoretical values of the ^{17}O quadrupolar coupling constant. This is true of both polymorphic forms. While the experimental values are both approximately −4.6 MHz, all of the calculated values are significantly larger in magnitude than this. For both the RHF and DFT methods, the value of C_Q generally decreases as the size of the basis set is increased. Still, for an RHF calculation with the 6-311++G** basis set on all atoms, the calculated value of −6.13 MHz is 33% larger than the experimental value of −4.6 MHz.

An increasingly common practice in the literature is the use of *calibrated* ^{17}O nuclear quadrupole moments,[109,122−124] instead of the accepted experimental value of −25.58(22) mb.[75,76] This method supposedly allows for the accurate calculation of oxygen-17 nuclear quadrupolar coupling constants even at modest levels of theory. Nevertheless, even using one of the smallest calibrated values for $Q(^{17}O)$ (−22.9 mb for RHF/3-21G calculations)[123] still results in a C_Q which is substantially greater than the experimental value, e.g., −7.20 MHz (calcd) vs −4.57 MHz (exptl) for the monoclinic

(113) Schindler, M.; Kutzelnigg, W. *J. Chem. Phys.* **1982**, *76*, 1919−1933.
(114) Cornet, R.; Landsberg, B. M.; Winnewisser, G. *J. Mol. Spectrosc.* **1980**, *82*, 253−263.
(115) Jameson, C. J. In *Specialist Periodical Reports*; Webb, G. A., Ed.; Royal Society of Chemistry: London, 1989; Vol. 18, Chapter 1.
(116) Malli, G.; Froese, C. *Int. J. Quantum Chem.* **1967**, *1S*, 95−98.
(117) Cameron, T. S. Unpublished results.
(118) Ishii, Y.; Terao, T.; Hayashi, S. *J. Chem. Phys.* **1997**, *107*, 2760−2774.
(119) Carravetta, M.; Eden, M.; Johannessen, O. G.; Luthman, H.; Verdegem, P. J. E.; Lugtenburg, J.; Sebald, A.; Levitt, M. H. *J. Am. Chem. Soc.* **2001**, *123*, 10628−10638.
(120) Ishii, Y. *J. Chem. Phys.* **2001**, *114*, 8473−8483.
(121) Case, D. A. *J. Biomol. NMR* **1999**, *15*, 95−102.
(122) Eggenberger, R.; Gerber, S.; Huber, H.; Searles, D.; Welker, M. *J. Mol. Spectrosc.* **1992**, *151*, 474−481.
(123) (a) Ludwig, R.; Weinhold, F.; Farrar, T. C. *J. Chem. Phys.* **1995**, *103*, 6941−6950. (b) Ludwig, R.; Weinhold, F.; Farrar, T. C. *J. Chem. Phys.* **1996**, *105*, 8223−8230.
(124) De Luca, G.; Russo, N.; Köster, A. M.; Calaminici, P.; Jug, K. *Mol. Phys.* **1999**, *97*, 347−354.

Table 2. Ab Initio Calculations of the Oxygen Electric Field Gradient and Nuclear Magnetic Shielding Tensors in Orthorhombic Triphenylphosphine Oxide (Polymorph A)

method	basis set[a]	C_Q/MHz	η	σ_{iso}/ppm	δ_{iso}/ppm	Ω/ppm	κ
RHF	3-21G	−8.28	0.02	327.7	−40.2	203	−0.84
RHF	6-311G	−10.7	0.02	339.5	−52.0	249	−0.74
RHF	6-311+G*	−6.41	0.02	290.3	−2.8	139	−0.59
RHF	6-311++G** on all atoms	−6.34	0.02	284.0	3.5	143	−0.60
DFT/B3LYP	3-21G	−7.19	0.01	270.2	17.3	243	−0.84
DFT/B3LYP	6-311G	−9.55	0.01	273.0	14.5	277	−0.75
DFT/B3LYP	6-311+G*	−5.99	0.01	250.0	37.5	173	−0.60
DFT/B3LYP	6-311++G** on all atoms	−5.95	0.01	242.4	45.1	180	−0.53
expt		−4.59 ± 0.01	<0.01	242.4	45.1 ± 0.2	135 ± 3	−0.76 ± 0.03

[a] Basis sets were applied to phosphorus, oxygen, and the carbon atoms directly bound to phosphorus. The 3-21G basis set was used on all remaining atoms unless otherwise indicated.

Table 3. Ab Initio Calculations of the Oxygen Electric Field Gradient and Nuclear Magnetic Shielding Tensors in Monoclinic Triphenylphosphine Oxide (Polymorph B)

method	basis set[a]	C_Q/MHz	η	σ_{iso}/ppm	δ_{iso}/ppm	Ω/ppm	κ
RHF	3-21G	−8.04	0.05	321.6	−34.1	214	−0.99
RHF	6-311G	−10.5	0.05	331.9	−44.4	273	−0.87
RHF	6-311+G*	−6.17	0.05	280.1	7.4	167	−0.78
RHF	6-311++G** on all atoms	−6.13	0.05	275.2	12.3	169	−0.77
DFT/B3LYP	3-21G	−6.95	0.04	259.6	27.9	263	−0.97
DFT/B3LYP	6-311G	−9.27	0.04	260.1	27.4	310	−0.88
DFT/B3LYP	6-311+G*	−5.74	0.05	235.8	51.7	208	−0.79
DFT/B3LYP	6-311++G** on all atoms	−5.70	0.05	228.2	59.3	211	−0.80
expt		−4.57 ± 0.01	0.030 ± 0.002	234.5	53.0 ± 0.2	155 ± 5	−0.75 ± 0.02

[a] Basis sets were applied to phosphorus, oxygen, and the carbon atoms directly bound to phosphorus. The 3-21G basis set was used on all remaining atoms unless otherwise indicated.

form of Ph_3PO. Thus the experimental value of Q which we have employed is not likely a major cause for the observed discrepancy between the experimental and calculated values of C_Q. Most of the discrepancy probably arises from intermolecular effects in the solid state. To our knowledge, no experimental gas-phase value of $C_Q(^{17}O)$ is available for any phosphine oxides; a microwave study on H_3PO with ^{17}O in only natural abundance (0.038%) has been carried out.[125] All the calculations reported herein are for isolated molecules; thus, a direct comparison with the experimental solid-state data is not expected to give quantitative agreement. Nevertheless, the small but significant difference in η for the two polymorphs (<0.01 vs 0.030) is reproduced by the calculations. The calculated value of η is consistently larger for the monoclinic form, regardless of the method and basis set used. We note that a recently measured highly precise value of $C_Q(^{17}O)$ for carbon monoxide may lead to an improved value of the ^{17}O nuclear quadrupole moment.[126]

Use of our recently revised experimental oxygen absolute shielding scale[74] enables the comparison between calculated nuclear magnetic shielding constants and experimental chemical shifts. The agreement between the experimental and calculated isotropic chemical shifts shown in Tables 2 and 3 is very good for both polymorphs. In particular, the B3LYP/6-311++G** calculations perform very well. It is satisfying that both the RHF and DFT calculations consistently indicate that the monoclinic form should exhibit a larger isotropic chemical shift, which it does, especially given the relatively small difference in the experimental chemical shifts for the two polymorphs, about 8 ppm. The span of the oxygen chemical shift tensor is calculated with reasonable accuracy for both polymorphs; e.g., at the RHF/6-311++G** level, the span is calculated to be 143 ppm for the orthorhombic form, compared with the experimental value of 135 ± 3 ppm. Importantly, the calculations consistently predict a larger span for the monoclinic form, as is the case experimentally. The skew of the oxygen CS tensor, about −0.75 for both polymorphs, is reproduced with good accuracy by all of the calculations. For example, the B3LYP calculation with the 6-311G basis set gives a value of −0.75 for the orthorhombic form and −0.88 for the monoclinic form.

The absolute orientations of the ^{17}O CS tensors in the molecular framework, for both polymorphs, determined at the RHF/6-311++G** level, are depicted in Figure 9. For the monoclinic form, the orientation of the EFG tensor is also shown. Since the asymmetry of the EFG tensor for the orthorhombic form is zero, the V_{XX} and V_{YY} components are equal and their orientations in the plane perpendicular to the PO bond are meaningless. The calculated Euler angles which define the rotations required to bring the PAS of the EFG tensor into coincidence with that of the CS tensor are as follows: $\alpha = 66.5°$, $\beta = 84.1°$, $\gamma = 5.9°$ (monoclinic); $\beta = 86.6°$, $\gamma = 6.8°$ (orthorhombic). In both cases, the δ_{11} and V_{ZZ} components are approximately along the phosphorus−oxygen internuclear axis. It is possible to compare the experimental and calculated relative orientations of the EFG and CS tensors by comparing the Euler angles reported in Table 1 with the calculated values given above. The agreement is very good for all of the angles. Direction cosines

(125) Ahmad, I. K.; Ozeki, H.; Saito, S. *J. Chem. Phys.* **1999**, *110*, 912−917.
(126) Cazzoli, G.; Dore, L.; Puzzarini, C.; Beninati, S. *Phys. Chem. Chem. Phys.* **2002**, *4*, 3575−3577.

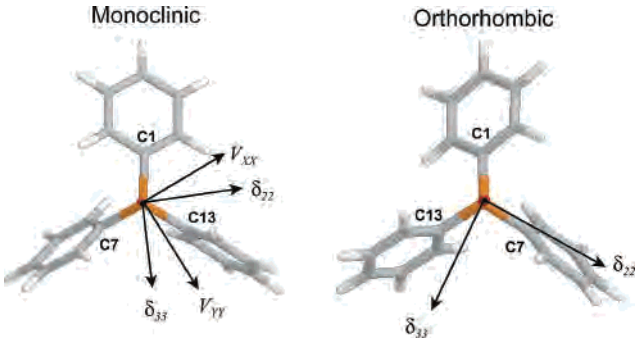

Figure 9. Calculated (RHF/6-311++G**) orientations of the ^{17}O chemical shift tensors for monoclinic and orthorhombic triphenylphosphine oxide. Also shown is the orientation of the ^{17}O EFG tensor for the monoclinic polymorph. The molecules are oriented such that the P−O bond is perpendicular to and above the plane of the page. In both cases, the δ_{11} and V_{ZZ} components are approximately along the P−O internuclear axis and thus the remaining components lie approximately in the plane of the page. The *ipso* carbon atoms are labeled according to the scheme of reference 42. The Euler angles required the bring the PAS of the EFG tensor into coincidence with the PAS of the CS tensor at this level of theory are the following: $\alpha = 66.5°$, $\beta = 84.1°$, $\gamma = 5.9°$ (monoclinic); $\beta = 86.6°$, $\gamma = 6.8°$ (orthorhombic). See the Supporting Information for further details.

Table 4. Ab Initio and Density Functional Theory Calculations of $\mathbf{J}(^{31}P, ^{17}O)$ in Phosphine Oxides[a]

method	basis set	$J_{iso}(^{31}P,^{17}O)$/ Hz	$\Delta J(^{31}P,^{17}O)$/ Hz
DFT/ZORA (scalar) GGA	ADF-ZORA IV	+231	−274
DFT/ZORA (scalar) GGA	ADF-ZORA V	+232	−279
DFT/ZORA (scalar) GGA[b]	ADF-ZORA V	+214	−248
DFT/ZORA (scalar) GGA[c]	ADF-ZORA V	+205	−236
DFT/ZORA (spin−orbit) GGA	ADF-ZORA IV	+230	−272
DFT/ZORA (spin−orbit) GGA	ADF-ZORA V	+231	−278
MCSCF CAS (52/51)	cc-pVTZ	+193	−306
MCSCF CAS (52/51)	aug-cc-pVTZ	+154	−294
MCSCF CAS (52/51)	cc-pVQZ	+181	−311
MCSCF RAS (52/52/00/51)	cc-pVTZ	+172	−254
MCSCF RAS (52/52/00/51)	aug-cc-pVTZ	+138	−240
MCSCF RAS (95/52/00/51)	cc-pVTZ	+184	−252
expt[d]		81−220	
expt ($Ph_3P^{17}O$ in solid state)		+150 ± 20	(<−600)[e]

[a] All calculations were done on H_3PO at the MP2/6-311+G* optimized geometry unless otherwise indicated. [b] Calculation on $(CH_3)_3PO$ at the MP2/6-311+G* optimized geometry. [c] Calculation on Ph_3PO using atomic coordinates from the X-ray structure for the monoclinic form. [d] Known range of $^1J_{iso}(^{31}P, ^{17}O)$ values. [e] Estimated upper limit. See text.

relating the calculated tensor orientations to the orthogonalized crystal frames are available as Supporting Information.

(b) Phosphorus−Oxygen Indirect Nuclear Spin−Spin Coupling Tensor. Shown in Table 4 are the results of MCSCF and DFT calculations of the phosphorus−oxygen indirect nuclear spin−spin coupling tensor, $^1\mathbf{J}(^{31}P, ^{17}O)$ for phosphine oxide, H_3PO. Some values are also presented for trimethylphosphine oxide and Ph_3PO (monoclinic). All of the MCSCF values of J_{iso} are in reasonably good agreement with the experimental value for the solid triphenylphosphine oxide polymorphs, +150 ± 20 Hz. Furthermore, all values lie within the known range of values for $J_{iso}(^{31}P,^{17}O)$ in phosphine oxides and related systems containing a terminal P−O moiety, 81−220 Hz. In addition to providing a positive isotropic value of **J**, the calculations also furnish the complete tensor properties, i.e., ΔJ, η_J, and the orientation of the **J** tensor in the molecular framework. Both the MCSCF and DFT calculations predict a value for ΔJ of around −300 Hz; all of the values in Table 4 lie within the experimental range estimated in the previous section. The calculated value of η_J is 0.00 for all calculations on H_3PO; this is required on the basis of the C_{3v} symmetry about the P−O bond axis. Both the MCSCF and DFT calculations show that the FC mechanism is the largest contributor to $\mathbf{J}(^{31}P,^{17}O)$; e.g., it accounts for 75% of the coupling at the RAS/aug-cc-pVTZ level. The PSO mechanism is the next most important contributor; for example, 24% at the RAS/aug-cc-pVTZ level and 16% for the DFT calculations. The overestimation of J_{iso} by the DFT calculations compared to the experimental data and the MCSCF calculations arises from an overestimate of the ZORA combined FC + SD contribution. Both methods indicate that the SD and DSO mechanisms contribute very little to the calculated coupling tensor.

Conclusions

This study has provided a definitive ^{17}O solid-state NMR characterization of the oxygen environment in two triphenylphosphine oxide polymorphs. In particular, the oxygen chemical shift tensor, as well as the quadrupolar asymmetry parameter, is found to be especially indicative of polymorphism. In contrast, the ^{17}O nuclear quadrupolar coupling constants are identical within error for the monoclinic and orthorhombic modifications. In general, CS tensors are most sensitive to the local environment while EFG tensors are much more dependent on long-range effects. On this basis it is tempting to suppose that the quadrupolar parameters should be more sensitive to polymorphism than the CS tensor; nevertheless in the present study the opposite is true.

The relatively small span of the oxygen CS tensor and highly shielded isotropic chemical shift are due to a lack of significant paramagnetic contributions to the shielding tensor, which in turn is due to a lack of low-lying virtual orbitals of appropriate symmetry. Such a situation could arise in the absence of significant π-bonding between phosphorus and oxygen. The oxygen CS tensor, as well as the small (compared to carbonyl oxygens) ^{17}O nuclear quadrupolar coupling constant, therefore tends to favor the polarized singly σ-bonded representation of phosphine oxides, $R_3P^+-O^-$. This view is also bolstered by the large dipole moments observed for phosphine oxides (e.g., 4.39 D in $(CH_3)_3PO$)[127] compared to, e.g., formaldehyde (2.33 D).

In general, ab initio and DFT calculations of the ^{17}O EFG and nuclear magnetic shielding tensors reproduce the differences seen experimentally between the two polymorphs. In combination with the experimental data, the calculations also allow for the proposal of the absolute orientations of the EFG and CS tensors in the molecular framework. New insights into the properties of the $\mathbf{J}(^{31}P,^{17}O)$ tensor have been provided by high-level ab initio and DFT calculations. Importantly, the calculations suggest that the magnitude of ΔJ is greater than the isotropic coupling constant. The large anisotropy in **J** arises primarily from the Fermi-contact−spin-dipolar coupling mechanism, with contributions from

(127) Armstrong, R. S.; Aroney, M. J.; Le Fèvre, R. J. W.; Pierens, R. K.; Saxby, J. D.; Wilkins, C. J. *J. Chem. Soc. A* **1969**, 2735−2739.

the paramagnetic spin−orbit mechanism, despite the fact that J_{iso} is predominantly governed by the Fermi-contact mechanism.

Acknowledgment. The authors thank the solid-state NMR group at the University of Alberta and Dr. Mike Lumsden and Brian Millier at Dalhousie University for many helpful comments and technical assistance. We thank Prof. T. Stan Cameron, Dr. Robert McDonald, and Dr. Michael Ferguson for the X-ray crystallographic studies. We thank the Natural Sciences and Engineering Research Council (NSERC) of Canada for research grants. Some spectra were acquired at the Atlantic Region Magnetic Resonance Centre, which is supported by NSERC. R.E.W. holds a Canada Research Chair in physical chemistry at the University of Alberta. D.L.B. thanks NSERC, the Izaak Walton Killam Trust, and the Walter C. Sumner Foundation for postgraduate scholarships. K.E. thanks Dr. Ulrich Fleischer for invaluable discussions on magnetic shieldings.

Supporting Information Available: A table of orientations (direction cosines) of the ^{17}O and ^{31}P nuclear magnetic shielding tensors and ^{17}O electric field gradient tensors in the orthogonalized crystal frame calculated at the RHF/6-311++G** level for two polymorphs of triphenylphosphine oxide. This material is available free of charge via the Internet at http://pubs.acs.org.

IC020706P